HHS Public Access

Author manuscript

Cancer Lett. Author manuscript; available in PMC 2022 February 01.

Published in final edited form as:

Cancer Lett. 2021 February 01; 498: 1–18. doi:10.1016/j.canlet.2020.09.010.

Negative Cross talk between LIMK2 and PTEN promotes Castration Resistant Prostate Cancer Pathogenesis in cells and in vivo

Kumar Nikhil[#], **Mohini Kamra**[#], **Asif Raza**, **Kavita Shah**[*]

Department of Chemistry and Purdue University Center for Cancer Research 560 Oval Drive, West Lafayette, IN 47907

Abstract

Androgen deprivation therapy (ADT) and androgen receptor (AR) signaling inhibitors are front-line treatments for highly aggressive prostate cancer. However, prolonged inhibition of AR triggers a compensatory activation of PI3K pathway, most often due to the genomic loss of tumor suppressor PTEN, driving progression to the castration-resistant prostate cancer (CRPC) stage, which has very poor prognosis. We uncovered a novel mechanism of PTEN downregulation triggered by LIMK2, which contributes significantly to CRPC pathogenesis. LIMK2 is a CRPC-specific target. Its depletion fully reverses tumorigenesis in vivo. LIMK2 phosphorylates PTEN at five sites, degrading and inhibiting its activity, thereby driving highly aggressive oncogenic phenotypes in cells and in vivo. PTEN also degrades LIMK2 in a feedback loop, which was confirmed in prostates from $PTEN^{-/-}$and $PTEN^{+/+}$ mice. LIMK2 is also the missing link between hypoxia and PTEN degradation in CRPC. This is the first study to show a feedback loop between PTEN and its regulator. Uncovering the LIMK2-PTEN loop provides a powerful therapeutic opportunity to retain the activity and stability of PTEN protein by inhibiting LIMK2, thereby halting the progression to CRPC, ADT-resistance and drug-resistance.

Keywords

LIMK2; PTEN; Castration resistant prostate cancer; EMT; PI3K; AKT

Introduction

Prostate cancer (PCa) is the second most common cancer in men in the U.S. The two first-line treatments are either surgical castration or androgen deprivation therapy (ADT)

[*]To whom correspondence should be addressed shah23@purdue.edu.

[#]Both authors contributed equally

Authors' contributions: KN and MK conducted most of the experiments. AR generated PTEN mutants and conducted kinase assays; KS conceived the idea, supervised the project and wrote the manuscript with input from all authors.

Conflict of Interest

The authors declare no conflict of interest.

(1), which are initially effective, but are palliative options (2,3). Eventually, most patients progress to the castration resistant prostate cancer (CRPC) stage, which has very poor prognosis. This study uncovered a novel molecular mechanism of CRPC pathogenesis triggered by LIMK2, a dual specificity kinase. LIMK2 regulates actin dynamics in normal cells by phosphorylating cofilin (4). It is overexpressed in many cancers and is associated with enhanced tumorigenesis and metastasis (5–7). We recently showed that LIMK2 is a disease-specific target in PCa, which is specifically upregulated in response to castration in mice due to increased hypoxia (8). Further, using a cohort of 156 clinical specimens, we observed that LIMK2 levels were highest in CRPC human tissues compared to other stages of PCa. LIMK2 was minimally expressed in normal prostates. Most importantly, inducible knockdown of LIMK2 fully reversed tumorigenesis in nude mice, underscoring the potential of LIMK2 as a clinical target for CRPC (8). Despite these findings, the molecular mechanisms by which LIMK2 contributes to oncogenesis remain largely unknown, as only three LIMK2 substrates have been identified to date.

At the molecular level, androgen receptor (AR) signaling is a key driver for all stages of PCa, including CRPC (9, 10). The androgen signaling inhibitors, abiraterone and enzalutamide, are beneficial initially, but persistent inhibition of AR signaling in CRPC patients triggers a compensatory adaptive activation of the PI3K pathway, which drives drug resistance (11). Phosphatase and tensin homologue (PTEN), a tumor suppressor, is often lost or mutated in up to 70% of CRPC patients, which is the major mechanism that hyperactivates PI3K pathway (12, 13). PTEN is primarily a lipid phosphatase but can also serve as a protein phosphatase (14, 15). PTEN null cells are intrinsically susceptible to CRPC and highly resistant to ADT (16, 17). Loss of PTEN aberrantly activates PI3K-AKT pathway, which is strongly associated with CRPC progression, poor prognosis, and high tumor recurrence in patients treated with radical prostatectomy (18) or abiraterone (19). While there are numerous reports of genomic aberrations of PTEN, relatively few of those have reported its downregulation at a post-translational level.

Since our previous findings showed that LIMK2 is particularly upregulated in CRPC tissues, we investigated whether LIMK2 contributes to PI3K signaling in CRPC pathogenesis. This study unveiled that PTEN and LIMK2 are engaged in a direct negative reciprocal loop, which drives upregulation of PI3K pathway and highly aggressive oncogenic phenotypes in CRPC cells as well as in vivo.

Materials and Methods

Antibodies and Cell lines

PC3, HEK293T, 22Rv1 and Phoenix cells were purchased from ATCC. LNCaP-95 (LN95) cells were kind gift from Professor Jun Luo. All antibodies used in this study were bought from Santa Cruz Biotech. All validated antibodies were used at 1–1000 dilution. Antibodies details are provided in Supplementary Table 1.

LIMK2 and PTEN shRNAs

The details of LIMK2 shRNAs was shown in our previous study (7). pLKO-PTEN-shRNA-1320 was a gift from Todd Waldman (20). Scrambled, LIMK2 and PTEN shRNA lentiviruses were generated and used to infect PC3, LN95 and 22Rv1 cells. Puromycin selection was employed to generate corresponding stable cell lines.

Site Directed Mutagenesis, expression and purification of LIMK2, WT and PTEN mutants

1066 pBabe puroL PTEN was a gift from William Sellers. Using it as a template, we generated HA-tagged PTEN and cloned into pBabe and TAT-HA vectors at BamHI and EcoR1 sites. Various phospho-dead mutants of PTEN were generated using site-directed overlap PCR. 6x-His tagged recombinant WT and mutant PTEN proteins were produced in *E. coli* and purified using Ni-NTA beads as we reported before (21). LIMK2 was produced in insect cells as reported before (8).

In vitro Kinase Assays

In vitro phosphorylation of 6x-His-fused WT or phospho-dead mutants of PTEN were performed for 30 min using LIMK2 and 0.5 μCi of [$\gamma-^{32}$P]ATP as reported before (22, 23). The proteins were separated by SDS-PAGE gel, transferred to PVDF membrane and exposed for autoradiography.

Ubiquitylation assay

6x-His-ubiquitin expressing 22Rv1 cells were infected with LIMK2, WT or PTEN mutant retrovirus for 36h. 10 μM MG132 (Sigma) was next added for an additional 12h as reported before (24). Following cell lysis, ubiquitylated proteins were immunoprecipitated using substrate-specific antibodies, followed by 6x-His IB.

Chemotaxis assay

Chemotaxis assays were performed in triplicates, three independent times as we reported before (24). Briefly, serum-starved cells (treated with 0.2% FBS for 16h) were isolated by limited trypsin digestion. 200 μl of full growth media was added to the lower compartment of Boyden chambers followed by placing of Whatman® Nuclepore™ Track-Etched Membrane and sealing the chamber using retainers. Suspended cells (10^3 cells in 200 μl serum free DMEM) were added to the top compartment onto the membrane. After 4h at 37°C, the inner surface of the chamber was cleaned with a cotton applicator and the membranes were recovered from the chambers. Cells were counted using 10 random frames under AmScope inverted light microscope. The data were normalized to number of seeded cells and are expressed as percentage cell numbers that migrated on the membrane. Multiple assays were performed and plotted for obtaining statistical significance.

MTT assay

MTT assay was performed as reported before (25). Experiments were repeated three independent times in triplicate.

Immunofluorescence

22Rv1 cells were grown on poly-L-lysine coated coverslips. Following treatments, they were fixed using 4% formaldehyde and subsequently washed with PBS (3x). Following their incubation in blocking buffer (1%FBS, 2% BSA, 0.1% triton X-100 in PBS), they were exposed to PTEN, HA or LIMK2 antibodies for 12 hours, followed by fluorescein-isothiocyanate-conjugated secondary antibody and DAPI staining. Cells were imaged using Nikon Eclipse E600 microscope (Nikon Instruments, Melville, NY).

LIMK2 Inhibitor treatment

LIMK2 inhibitor-*N*-benzyl-*N*-methyl-4-(N-phenylsulfamoyl)benzamide was synthesized as published before (26). It was used at 10 μM concentration as detailed in Figure legends.

qPCR Assay

qPCR was conducted as we reported before (8). qPCR primer sequences are included in Supplementary Table 2.

Lipid Phosphatase Activity

Lipid phosphatase activity of PTEN was measured using phosphatidylinositol 3,4,5 trisphosphate (PIP3) as the substrate and malachite green as the colorimetric readout (27). WT and mutant PTEN proteins (either immunoprecipitated from 22Rv1 cells or expressed and purified from SF9 cells) were incubated with 50 μM PIP3 in phosphatase buffer (25 mM Tris and 100 mM NaCl pH 7.6) in a final reaction volume of 50 μL. The reaction mixture was incubated at 37 °C for 30 min, followed by addition of 50 μL malachite green to stop the reaction. The release of inorganic phosphate was quantified by measuring the absorbance at 620 nm over a period of 1h using Tecan microplate reader. To measure the consequences of LIMK2-mediated phosphorylation on PTEN activity, it was phosphorylated using LIMK2 in kinase buffer (37.5 mM Hepes pH 8, 300 μM ATP, 4 mM $MgCl_2$) for 30 min followed by PTEN phosphatase assay. For the dephosphorylation experiment, PTEN activity was measured for 30 min, after which 1 μL of calfalkaline phosphatase was added to the sample and the measurements were performed for another 30 min. For untreated samples, 50% glycerol in 1x CutSmart Buffer (New England Biolabs) was added as a control.

Hypoxia

Control or infected cultures were placed in a modular hypoxia chamber containing 1% oxygen, 5% CO_2, and 94% nitrogen gas mixture for 12h, after which the chamber was re-gassed with hypoxic gas. The cells were then incubated for an additional 12h. For chemical-induced hypoxia experiments, 22Rv1 cells were treated with 100 μM cobalt chloride 30 min prior to the addition of LIMK2 inhibitor. The cells were then incubated for an additional 24h. For inducing hypoxia in LIMK2 shRNA-treated cells, 22Rv1 cells were first treated with either scrambled shRNA or LIMK2 shRNA for 18h, followed by the addition of 100 μM cobalt chloride for an additional 24h.

Soft agar colony formation

Soft agar assay was performed in triplicate as reported before (28).

In vivo xenograft in nude mice

All animal experiments and animal care were done in accordance with Purdue University institutional guidelines (PACUC) using an approved protocol # 1111000292. 4 weeks old male athymic nude mice were obtained from Taconic Laboratories and injected as before (8). Tumor bearing mice exhibited no weight loss compared with control mice. The animals were euthanized 22 days after tumor injection, tumor tissues were isolated and flash-frozen in liquid nitrogen.

Statistical analysis

Data are expressed as mean±s.e.m. and were statistically evaluated with oneway ANOVA followed by the Bonferroni post hoc test using GraphPad Prism 5.04 software (GraphPad Software). $P<0.05$ was considered statistically significant.

Results

LIMK2 upregulates PI3K pathway via PTEN degradation in CRPC cells

To examine whether LIMK2 affects PI3K signaling pathway, we ectopically expressed LIMK2 in castration-resistant 22Rv1 cells and analyzed phospho-AKT levels at S473 and T308 sites. LIMK2 overexpression increased AKT activation as depicted by increased phosphorylation at both sites (Figure 1A). The effect of LIMK2 overexpression on phospho-AKT levels from three independent experiments is demonstrated in Figure 1B. Similarly, LIMK2 knockdown decreased phospho-AKT levels at S473 and T308 sites (Figure 1C, D). As a control, we also analyzed total AKT levels, which showed no discernable change upon LIMK2 overexpression or knockdown (Supplementary Figure 1A, B). In parallel, phospho-cofilin levels were analyzed as a positive control, which revealed increased phosphorylation upon LIMK2 overexpression, and reduced upon its knockdown as expected (Supplementary Figure 1A, B). We further inhibited LIMK2 using a LIMK2-specific inhibitor (26), which too inhibited AKT activation, thereby confirming a positive role of LIMK2 in regulating AKT signaling (Figure 1E, F).

Our previous studies showed that hypoxia upregulates LIMK2 transcription (8). As AKT pathway is also activated upon hypoxia, we investigated whether LIMK2 was a probable cause. Initially, hypoxia was induced by treating 22Rv1 cells with cobalt chloride, a hypoxia mimetic, which showed significant increase in AKT phosphorylation at S473 and T308 sites (Supplementary Figure 1C, D). More importantly, when LIMK2 was knocked-down, it significantly diminished hypoxia-induced AKT activation, indicating that LIMK2 likely activates AKT under hypoxic conditions (Supplementary Figure 1C, D). To confirm this finding, we exposed 22Rv1 cells to hypoxic conditions using 1% oxygen for 24h, and measured AKT phosphorylation. We observed over three-fold increase in AKT phosphorylation at S473 and T308 sites (Figure 1G, H), which confirms a key role of LIMK2 in activating AKT upon hypoxia.

In an effort to deconvolute the molecular mechanism of AKT regulation by LIMK2, we focused on PTEN and analyzed whether it serves as a link between LIMK2 and AKT. We overexpressed LIMK2 in 22Rv1 cells, which led to robust downregulation of PTEN (Fig.

1I, J). Likewise, LIMK2 knockdown resulted in concurrent upregulation of PTEN protein, confirming that LIMK2 negatively regulates PTEN (Figure 1K, L).

We next examined whether LIMK2 downregulates PTEN at the transcriptional level. LIMK2 was overexpressed in 22Rv1 cells, which showed a ~3.5-fold increase in its mRNA levels, but there was no change in PTEN mRNA levels (Figure 1M). Likewise, LIMK2 knockdown using corresponding shRNA was ineffective in altering PTEN mRNA levels (Figure 1N). These results indicated that LIMK2 most likely regulates PTEN post-translationally.

To test this hypothesis, we inhibited protein synthesis in 22Rv1 and LIMK2-overexpressing 22Rv1 (LIMK2–22Rv1) cells using cycloheximide for 10h and 20h (PTEN has a relatively long half-life) and analyzed PTEN levels. As shown in Figures 1O and 1P, LIMK2 overexpression indeed decreased PTEN stability in 22Rv1 cells. As LIMK2 has a short half-life (7, 8), it was fully degraded after 10h of cycloheximide treatment. To validate this finding, we also investigated the PTEN degradation rate in cycloheximide-treated 22Rv1 and LIMK2 shRNA-treated 22Rv1 cells. LIMK2 downregulation increased PTEN stability, thereby confirming that LIMK2 downregulates PTEN by decreasing its protein stability (Figures 1Q, R).

To test whether PTEN degradation was ubiquitin-dependent or ubiquitin-independent, LIMK2 was overexpressed in 6x-His-ubiquitin expressing 22Rv1 cells and PTEN ubiquitylation was analyzed. While control cells showed minimal ubiquitylation, LIMK2–22Rv1 cells showed robust PTEN ubiquitylation, confirming that LIMK2 promotes PTEN ubiquitylation (Figure 1S).

LIMK2 inhibits PTEN phosphatase activity in vitro and in cells

As PTEN is a lipid phosphatase, we next explored whether LIMK2 regulates PTEN enzymatic activity. As shown in Figures 2A and 2B, PTEN showed robust lipid phosphatase activity in an in vitro assay, which remained unaltered upon incubation with either ATP or LIMK2. However, when PTEN was phosphorylated using LIMK2 and ATP, it showed a significant decrease in its phosphatase activity, indicating that LIMK2 negatively regulates PTEN activity via phosphorylation. To confirm this finding, PTEN was phosphorylated using LIMK2 in duplicate. Both samples showed similar activities as expected (Figure 2C). After 30 min, one sample was treated with calf alkaline phosphatase (CIP) to induce dephosphorylation of PTEN, which significantly rescued its activity (Figure 2C). Figure 2D shows relative activities of phospho-PTEN with and without CIP treatment after 50 min. These data suggest that LIMK2 inhibits PTEN activity by direct phosphorylation.

To examine whether LIMK2 regulates PTEN activity in cells, 22Rv1 cells were treated with scrambled shRNA or LIMK2 shRNA for 36h. PTEN proteins were isolated and their activities evaluated. As LIMK2 depletion increases PTEN levels, a huge excess of cell lysates was used along with limiting amount of the antibody to ensure equal protein concentrations. LIMK2 knockdown significantly increased PTEN activity as compared to the activity in control cells (Figurea 2E and 2F). To differentiate between alternative mechanisms of LIMK2-mediated PTEN regulation-protein-protein interaction vs. kinase activity, we inhibited LIMK2 in cells for 3h and 6h, which significantly rescued PTEN

activity (Figure 2G, 2H), thus indicating that LIMK2 inhibits PTEN activity using its kinase activity in cells and *in vitro*.

LIMK2 does not regulate PTEN subcellular localization

PTEN is nuclear in primary cells but is cytoplasmic in cancer cells. The absence of nuclear PTEN serves as a prognostic indicator. Therefore, we investigated whether PTEN's subcellular localization was regulated by LIMK2 in 22Rv1 cells. As shown in Figures 2I and 2J, PTEN was predominantly cytoplasmic in 22Rv1 cells. Neither LIMK2 inhibition nor LIMK2 knockdown had any effect on PTEN's cytoplasmic residence, suggesting that LIMK2 does not control PTEN localization in cells. This result was further confirmed using subcellular fractionation, which showed no relative changes in PTEN levels in the cytoplasm and nucleus in control and LIMK2-depleted 22Rv1 cells (Figure 2K).

LIMK2 regulates PTEN upon hypoxia

PTEN loss is associated with increased hypoxia in several cancers. As LIMK2 is upregulated by hypoxia (8), we examined whether LIMK2 was the missing link between hypoxia and PTEN downregulation. Initially, 22Rv1 cells were exposed to hypoxia using cobalt chloride for 24h, which showed a substantial increase in LIMK2 levels and a consequent decrease in PTEN levels (Supplementary Figure 2A-D). More importantly, LIMK2 inhibition and knockdown under these conditions rescued PTEN levels (Supplementary Figure 2A-D). To confirm these findings, we further examined PTEN levels under hypoxic conditions in 22Rv1 cells, which drastically reduced PTEN levels. Both LIMK2 inhibition and depletion reversed hypoxia-induced loss of PTEN (Figures 2L-O), indicating that LIMK2 is a missing link between hypoxia and PTEN downregulation.

PTEN engages in a negative feedback loop with LIMK2

We recently showed that LIMK2 is involved in a positive feedback loop with its substrate TWIST1, where both increase each other's stability (8). This prompted us to examine whether PTEN regulates LIMK2 reciprocally. PTEN was overexpressed in 22Rv1 cells, which significantly decreased LIMK2 levels (Figure 3A). Figure 3B shows average LIMK2 levels in control and PTEN-overexpressing cells from three independent experiments. Similarly, PTEN knockdown resulted in a simultaneous increase in LIMK2 levels, suggesting that PTEN negatively influences LIMK2 levels (Figure 3C, 3D). To uncover whether PTEN influences LIMK2 stability, we treated 22Rv1, PTEN-overexpressing 22Rv1 (PTEN-22Rv1) and PTEN shRNA-treated 22Rv1 cells (PTEN shRNA-22Rv1) with cycloheximide to inhibit protein synthesis and analyzed the half-life of LIMK2. While PTEN upregulation drastically decreased the half-life of LIMK2, PTEN depletion increased it, indicating that PTEN destabilizes LIMK2 protein (Figures 3E and 3F).

The next step was to investigate whether LIMK2 degradation was ubiquitin or non-ubiquitin-dependent. PTEN was overexpressed in 6x-His-ubiquitin expressing 22Rv1 cells, and potential ubiquitylation of LIMK2 analyzed. PTEN overexpression led to a robust increase in LIMK2 ubiquitylation, indicating that PTEN degrades LIMK2 by increased ubiquitylation (Figure 3G).

We also examined whether PTEN regulates LIMK2's subcellular localization using PTEN shRNA. LIMK2's subcellular location remained unchanged in scrambled shRNA-treated and PTEN-depleted cells, indicating that similar to LIMK2, PTEN also does not regulate LIMK2's residence in cells (Figure 3H).

LIMK2 levels are higher in PTEN null prostates compared to PTEN$^{+/+}$ prostates

The negative regulation of LIMK2 by PTEN prompted us to investigate whether this relationship exists in vivo. We compared LIMK2 expression in prostate tissues from PTEN$^{+/+}$ and PTEN$^{-/-}$mice. As indicated, LIMK2 levels were higher in prostatic tissue from PTEN-knockout mice compared to prostate tissues from wild type controls (Figure 3I), confirming that PTEN indeed negatively regulates LIMK2 in vivo.

PTEN is directly phosphorylated by LIMK2 at five sites

Our data show that LIMK2 controls PTEN post-translationally, indicating that it is presumably due to phosphorylation. We thus generated 6x-His-tagged recombinant PTEN and incubated it with LIMK2 in an in vitro kinase assay, which revealed it to be a direct target of LIMK2 (Figure 4A).

LIMK2 is a dual-specificity kinase, which can phosphorylate Ser, Thr and Tyr. However, peptide library screens revealed that LIMK1, a LIMK family member, does not show a robust consensus site preference for its substrates (27). LIMK2 peptide substrate specificity remains unknown. Furthermore, only three LIMK2 substrates are known to date -cofilin, TWIST1 and MT1-MMP2. Although MT1-MMP was shown to be phosphorylated at tyrosine residue, the exact phosphorylation site(s) was not identified (30). Both TWIST1 and cofilin are shown to be phosphorylated at serine residues, which are followed by small amino acids such as alanine and glycine. We identified several such potential serine sites on PTEN. In addition, we also focused on those serine residues as potential sites that were followed by another serine residue (SS) as serine and alanine are known to occupy effectively the same volume in proteins. These criteria suggested S207, S226, S360, S361 and S362 as potential LIMK2 sites on PTEN. We initially mutated S360, S361 and S362 individually to the corresponding alanine residues, and exposed each of these single mutants to kinase assay with LIMK2. Each of these phospho-mutants showed reduced phosphorylation as compared to wild-type (Figure 4B), indicating that all three sites were phosphorylated by LIMK2. We generated the corresponding triple mutant (3A) (S360A, S361A and S362A) and subjected it to kinase assay along with other phospho-dead single mutants S207A and S226A. These results show that LIMK2 phosphorylates all five sites (Figure 4C). To determine whether LIMK2 phosphorylates any additional sites, we generated the corresponding quintuple phospho-dead mutant (5A), which showed minimal phosphorylation with LIMK2, indicating that LIMK2 phosphorylates PTEN at these five sites only (Figure 4D).

To address whether PTEN is phosphorylated by LIMK2 in cells, we used two approaches. First, a mobility shift assay was employed, which is based on the principle that phosphorylated species migrate slower than the corresponding unphosphorylated version. LIMK2 was inhibited in 22Rv1 cells for 8h, which resulted in increased mobility of PTEN

as compared to DMSO-treated control. When the time of LIMK2 inhibition was increased to 12h, it further increased the mobility of PTEN (Figure 4E), indicating that LIMK2 phosphorylates PTEN in cells. In the second approach, we isolated HA-tagged WT and 5A-PTEN from PTEN-22Rv1 and 5A-22Rv1 cells using HA IP, respectively, and analyzed their phosphorylation levels using phospho-Ser antibody. 22Rv1 cells were used as controls. While WT PTEN showed robust phosphorylation, 5A-PTEN exhibited drastically reduced phosphorylation, indicating that these sites are phosphorylated in cells (Figure 4F). Figure 4G shows average phospho-Ser levels on PTEN in these cells from three independent experiments. To confirm that the reduction in phospho-Ser levels on 5A-PTEN is due to LIMK2, we inhibited LIMK2 in 22Rv1, PTEN-22Rv1 and 5A-22Rv1 cells for 12h, isolated WT and 5A-mutant using HA antibody, and analyzed phospho-Ser levels. As observed earlier, WT PTEN-expressing cells exhibited robust PTEN phosphorylation, whereas mutant PTEN showed minimal phosphorylation in vehicle-treated cells. More importantly, LIMK2 inhibitor treatment reduced phosphorylation of WT to basal levels, whereas the phospho-levels of 5A-mutant remained unperturbed, confirming that LIMK2 phosphorylates PTEN at these sites (Figure 4H, I).

Although our results indicated that LIMK2 does not regulate PTEN's subcellular localization, we nevertheless examined whether 5A-PTEN mutant shows different subcellular residence compared to WT. As shown in Figures 4J and 4K (using PTEN and HA antibodies respectively), both wild-type and mutant PTEN showed similar subcellular localization, suggesting that LIMK2-mediated phosphorylation does not control PTEN location in PCa cells.

LIMK2-mediated phosphorylation is responsible for increased ubiquitylation and inhibition of PTEN activity, causing AKT activation

LIMK2 downregulates PTEN stability and inhibits its activity (Figures 1I-S and 2A-H). Therefore, we investigated whether either or both of these events were phosphorylation-dependent. We ectopically expressed HA-tagged wild-type (WT) and 5A-PTEN in 22Rv1 cells and analyzed their levels. 5A-PTEN-22Rv1 cells showed higher PTEN levels as compared to WT-expressing cells, signifying increased stability of the phospho-dead mutant (Figure 5A). Figure 5B depicts average levels of WT and 5A-PTEN from three independent experiments. Further, cycloheximide experiments using 22Rv1, WT PTTEn-22Rv1 and 5A-22Rv1 cells confirmed increased stability of 5A-PTEN compared to WT PTEN (Figure 5C, D). We further observed increased ubiquitylation of WT PTEN compared to 5A-PTEN, thereby validating that LIMK2 promotes PTEN's ubiquitylation via direct phosphorylation (Figure 5E).

We specifically isolated HA-tagged PTEN and 5A-PTEN from corresponding WT and 5A-PTEN-overexpressing 22Rv1 cells using HA antibody to examine whether these proteins show variable enzymatic activities. As 5A-mutant was expressed at higher levels compared to wild-type PTEN (Figures 5A, B), we used excess of cell lysate and limiting amount of HA antibody to extract equal amounts of proteins. As shown in Figures 5F and 5G, wild-type PTEN shows reduced activity compared to 5A-mutant, indicating that LIMK2-mediated phosphorylation of PTEN inhibits its activity in cells.

Our in vitro data indicated that PTEN lipid phosphatase activity is regulated by LIMK2-mediated phosphorylation (Figure 2A-D). To confirm this finding, we exposed 5A-PTEN to LIMK2-mediated phosphorylation *in vitro* and analyzed its activity. As a control, WT PTEN (wild-type PTEN) was included, which was inhibited by LIMK2-mediated phosphorylation (Figure 2A, B). While the activity of WT PTEN was significantly inhibited when exposed to LIMK2-mediated phosphorylation (Figure 5H, I), there was only minimal change in 5A-PTEN activity when exposed to LIMK2 and ATP in a kinase assay buffer (Figures 5J, K). These findings confirm that LIMK2-mediated direct phosphorylation of PTEN attenuates its activity.

The contribution of each of the five phosphorylation sites in regulating PTEN activity was investigated next. We generated the corresponding single mutants and ectopically expressed them in 22Rv1 cells along with WT PTEN and 5A-PTEN. The proteins were isolated using HA IP with excess of cell lysate and a limiting amount of antibody to ensure equal loading (Figure 5L). Each single mutant displayed higher activity as compared to WT, with 5A mutant showing maximal activity (Figure 5L).

As PTEN is a major inhibitor of AKT activation, we measured relative AKT phosphorylation levels at S473 and T308 sites in control 22Rv1, PTEN-22Rv1 and 5A-PTEN-22Rv1 cells. As shown in Figures 5M and N, while WT PTEN inhibited phospho-AKT levels, 5A-PTEN inhibited more significantly, indicating that LIMK2-mediated upregulation of AKT pathway is predominantly through PTEN downregulation.

LIMK2-mediated phosphorylation of PTEN contributes to aggressive oncogenic phenotypes in 22Rv1 cells

To determine the consequences of LIMK2-mediated phosphorylation of PTEN in regulating various oncogenic phenotypes, cell proliferation rates were measured in 22Rv1 cells expressing either vector, LIMK2, PTEN or 5A-PTEN. As expected, LIMK2 expression augmented cell proliferation, whereas WT PTEN attenuated it compared to control cells. Notably, 5A-PTEN decreased it the most, which was consistent with its increased levels and activity in cells (Figure 6A). To determine the contribution of LIMK2-PTEN loop in regulating cell proliferation, we ectopically overexpressed LIMK2 in vector, PTEN and 5A-PTEN-expressing 22Rv1 cells, and measured growth rates after 48h. LIMK2 overexpression led to a robust increase in proliferation rate of all three cell-types, indicating that while LIMK2-mediated PTEN phosphorylation is a key factor, other LIMK2-triggered molecular mechanisms exist that also contribute to increased growth rate (Figure 6B). This hypothesis was confirmed by knocking down LIMK2 in vector, PTEN and 5A-PTEN-expressing 22Rv1 cells, revealing concomitant decrease in growth rates of all cell lines (Figure 6C).

The relative contributions of WT and phospho-dead mutant were next examined under anchorage-independent growth conditions using a soft agar assay, which revealed robust inhibition of colony formation in 5A-PTEN expressing cells as compared to WT PTEN-expressing cells (Figure 6D). Similarly, mutant PTEN was more effective in inhibiting cell motility relative to WT PTEN (Figures 6E, F). When LIMK2 was overexpressed in PTEN and 5A-PTEN-22Rv1 cells, cell motility was rescued in both cell types, indicating that additional LIMK2-dependent pathways also contribute to LIMK2-induced chemotaxis

(Figures 6G, H). Similar conclusions were derived when LIMK2 was depleted in PTEN and 5A-PTEN-22Rv1 cells, which inhibited cell motility in both cell lines (Figures 6I, J). These findings suggest that while LIMK2-mediated PTEN phosphorylation is a major contributor to increased cell motility, LIMK2 overexpression in these cells also recruits other molecules to promote malignant phenotypes.

PTEN is known to directly associate with AR and promote its degradation (31). Therefore, we examined whether LIMK2-mediated phosphorylation of PTEN affects AR levels. AR levels were examined in 22Rv1, PTEN-22Rv1 and 5A-PTEN-22Rv1 cells, which showed significant decrease in AR levels in both WT and 5A-mutant expressing cells as expected (Figure 6K, L).

PTEN phosphorylation by LIMK2 may contribute to enzalutamide resistance. Enzalutamide treatment reduced cell viability, which was potentiated by the expression of WT PTEN and 5A-PTEN, with latter being more effective (Figure 6M). Similar results were obtained when cells were treated with LIMK2 inhibitor (Figure 6N). These results prompted us to examine a combination regimen of LIMK2 inhibitor and enzalutamide, which revealed a synergistic effect, with maximal toxicity observed in 5A-PTEN mutant-expressing cells (Figure 6O). These results highlight the significance of PTEN downregulation by LIMK2 in CRPC drug-resistance.

LIMK2-PTEN feedback loop in PTEN$^{-/-}$PC3 and LN95 cells

To further determine the consequences of PTEN phosphorylation by LIMK2, WT and 5A-PTEN were ectopically expressed in PTEN null PC3 cells. As observed for 22Rv1 cells, 5A-PTEN was expressed at higher levels as compared to WT PTEN (Figures 7A, B). Cycloheximide treatment of PC3 cells showed this increase was due to improved stability of the mutant (Figures 7C, D). Furthermore, LIMK2 overexpression led to enhanced ubiquitylation of WT as compared to mutant PTEN, confirming that LIMK2-mediated phosphorylation degrades PTEN via ubiquitylation (Figure 7E).

We next investigated the consequences of PTEN phosphorylation on different oncogenic phenotypes in PC3 cells. While LIMK2 overexpression increased cellular growth rate, both WT and 5A-PTEN suppressed it when compared with control cells. As expected, 5A-mutant had a more robust inhibitory impact on cell growth as compared to WT PTEN (Figure 7F). As observed previously in 22Rv1 cells, LIMK2 overexpression increased cell growth and its knockdown decreased cell growth in all three cell types (Figures 7G and H, respectively), indicating that LIMK2 employs multiple mechanisms to stimulate cell growth.

Further, ectopic expression of 5A-PTEN in PC3 cells almost fully inhibited colony formation under anchorage-independent growth conditions, whereas WT PTEN led to 70% inhibition (Figure 7I). Similarly, both WT and mutant PTEN largely inhibited cell motility in PC3 cells (Figures 7J, K), which was significantly rescued by LIMK2 overexpression (Figures 7L, M). LIMK2 knockdown further confirmed this observation (Figures 7N, O). Thus, LIMK2-mediated phosphorylation and degradation of PTEN is an important contributor to prostate malignancy.

We further investigated the crosstalk between LIMK2 and PTEN in a third CRPC cell line-LN95. LN95 is also a PTEN null cell line. Therefore PTEN was stably expressed in these cells, which were named as LN95(P). When LIMK2 was overexpressed, PTEN levels declined (Figure 8A, B), and when LIMK2 levels were depleted, PTEN levels soared (Figure 8C, D), confirming that LIMK2 negatively regulates PTEN in LN95 cells as well.

Cycloheximide-mediated inhibition of protein synthesis was employed to quantify the differences in the half-lives of PTEN in LN95(P) and LIMK2-overexpressing LN95(P) cells. As shown in Figures 8E and F, LIMK2 overexpression decreased the stability of PTEN in LN95(P) cells, as it did in 22Rv1 and PC3 cells. These results were validated using LIMK2 knockdown, which increased the stability of PTEN in LN95(P) cells (Figures 8G, H). Furthermore, LIMK2 overexpression increased the ubiquitylation of PTEN (Figure 8I).

We also measured the relative growth rates of LN95, LIMK2-LN95, PTEN-LN95 and 5A-PTEN-LN95 cells. LIMK2 overexpression increased the growth rate in LN95 cells as expected. While PTEN expression decreased the growth rate, 5A-PTEN was more effective in stalling it (Figure 8J). Similarly, 5A-PTEN inhibited cell migration more robustly as compared to WT-expressing cells, underscoring the importance of LIMK2-mediated regulation of PTEN in promoting aggressive phenotypes (Figure 8K).

Finally, we measured enzalutamide and LIMK2 inhibitor sensitivity in LN95, PTEN-LN95 and 5A-PTEN-LN95 cell lines individually and in combination. As observed before, 5A-expressing cells were most sensitive to LIMK2 inhibitor and enzalutamide both when added independently or in combination (Figure 8L). Together these results highlight the significance of LIMK2-mediated PTEN regulation in drug sensitivity.

PTEN phosphorylation and downregulation by LIMK2 promotes tumorigenesis and EMT in vivo

We investigated the consequences of PTEN phosphorylation by LIMK2 *in vivo* next. 22Rv1 and PTEN-22Rv1 cells were inoculated in left and right shoulders of nude mice, respectively. Once the tumors became palpable, they were measured every two days. As expected, 22Rv1 cells exhibited robust tumor formation as compared to WT PTEN-expressing cells (Figures 9A, B). More importantly, 5A-PTEN-expressing cells showed minimal tumorigenesis, thereby underscoring a key role of PTEN degradation via phosphorylation in promoting tumorigenesis (Figures 9C, D).

Our previous studies have shown that LIMK2 plays a critical role in promoting EMT (8). Therefore, we isolated tumors originating from 22Rv1 cells and PTEN-22Rv1 cells and analyzed the levels of E-cadherin, an epithelial marker and vimentin, a mesenchymal marker. As mice injected with 5A-PTEN cells did not show any tumors, they could not be analyzed. E-cadherin levels increased in PTEN-expressing tumors, as compared to control tumors in vivo, whereas vimentin levels decreased in PTEN-expressing tumors (Figure 9E). These findings prompted us to investigate other EMT markers in these tumors, which confirmed that PTEN indeed inhibits EMT in CRPC cells (Figures 9F, G). Finally, we examined LIMK2 levels in PTEN-overexpressing tumors, which showed decreased

expression of LIMK2 as compared to control tumor, confirming the negative relationship in vivo (Figures 9F, G).

Discussion

The loss of PTEN is the most frequently altered pathways in primary PCa. PTEN loss is also one of the critical factors that drives disease progression towards the CRPC stage. Although, in a vast majority of cases, PTEN is lost due to genomic deletion, a few studies have also shown its regulation at protein level via post-translational modifications (PTM) such as acetylation, ubiquitylation, oxidation and phosphorylation. PTEN contains an N-terminal phosphatidylinositol-4, 5-bisphosphate-binding domain (PBD, amino acids 1–6), which is critical for membrane localization and catalytic activity (32). PBD is followed by phosphatase domain (amino acids 7–185), C2 domain (186–351) and a C-terminal tail (352–403). The phosphatase and C2 domains form the catalytic core of PTEN, whereas C-terminal tail contains a PDZ binding domain (PDZ-BD), which is important for PTEN activity and stability (Figure 9H) (33). PTEN has been shown to be phosphorylated mainly at the C-terminal tail and C2 domain, which can regulate its stability and activity. Accordingly, Casein kinase 2 (CK2)-mediated phosphorylation of PTEN at S370 and S380-S385 cluster (S380, T383, T383, S385) at the C-terminal tail stabilizes PTEN by reducing its cleavage with caspase-3, although it reduces its activity presumably by forming a closed conformation (32, 34). In contrast, glycogen synthase kinase 3β (GSK3β)-mediated phosphorylation of PTEN at T366 degrades it (35). ROCK kinase phosphorylates PTEN exclusively at C2 domain (T223, S229, T319, T321), which is important for chemotaxis (36). Similarly, fyn-related kinase (FRK aka RAK) phosphorylates PTEN at Y336 in the C2 domain, which increases PTEN stability (37).

In this study, we identified LIMK2 kinase as a major regulator of PTEN's stability and phosphatase activity. More importantly, this is the first study that shows that PTEN is engaged in a negative feedback loop with its kinase, where both degrade each other. LIMK2 phosphorylates PTEN at five sites, leading to PTEN ubiquitylation and subsequent degradation (Figure 9I). Furthermore, LIMK2 also inhibits the phosphatase activity of PTEN via direct phosphorylation. Importantly, PTEN is known to be downregulated in hypoxic tumors, although the molecular player leading to its downregulation remains unclear. This study uncovered that LIMK2 upregulation upon hypoxia in PCa might be one of the mechanisms by which PTEN is downregulated. Therefore, as LIMK2 levels increase under hypoxic conditions during CRPC progression (8), it might tilt the balance in favor of heightened PTEN degradation and inhibition, leading to aggressive oncogenic phenotypes including enzalutamide resistance. Accordingly, we observed that while WT PTEN expressing cells formed much smaller tumors compared to 22Rv1 cells, 5A-PTEN-expressing cells completely abrogated tumorigenesis, reinforcing the clinical significance of LIMK2-mediated regulation of PTEN.

Uncovering the upstream regulators of PTEN provides powerful therapeutic opportunities to retain the activity and stability of PTEN, thereby halting the progression of many fatal cancers, including CRPC. This study revealed LIMK2 as one such target. Its inhibition should be effective in not only inhibiting or delaying disease progression but also in

effectively reversing cancer phenotypes. Similarly, identification of PTM of PTEN could serve as prognostic and diagnostic biomarkers to predict the likelihood of therapeutic response for CRPC patients.

Supplementary Material

Refer to Web version on PubMed Central for supplementary material.

Acknowledgments:

pLKO-PTEN-shRNA-1320 was a gift from Todd Waldman (Addgene plasmid # 25638; http://n2t.net/addgene:25638; RRID:Addgene_25638). (29). 1066 pBabe puroL PTEN was a gift from William Sellers (Addgene plasmid # 10785; http://n2t.net/addgene:10785; RRID:Addgene_10785). We would like to thank Professor Xiaoqi Liu (UKY) for providing prostate slides from $PTEN^{+/+}$ and PTEN null mice and Professor Jun Luo (Johns Hopkins) for LN95 cells.

Funding: This work was supported by NSF award # 1708823, NIH-1R01-CA237660 and U.S. Army Medical Research Acquisition Activity, Prostate Cancer Research Program (Award # PC130391).

List of abbreviations:

LIMK2	LIMK Kinase 2
CRPC	Castration resistant prostate cancer
ADT	androgen-deprivation therapy
AR	androgen receptor
CR	castration resistant
PTEN	Phosphatase and tensin homologue
EMT	Epithelial to mesenchymal transition
PI3K	phosphoinositide 3-kinase
CHX	Cycloheximide

References

1. Sharifi N, Gulley JL, Dahut WL, Androgen deprivation therapy for prostate cancer. JAMA. 294(2) (2005), 238–44. [PubMed: 16014598]
2. Beer TM, Armstrong AJ, Rathkopf DE, Loriot Y, Sternberg CN, Higano CS et al. , Enzalutamide in metastatic prostate cancer before chemotherapy. N Engl J Med. 371(5) (2014), 424–33. [PubMed: 24881730]
3. Ryan CJ, Molina A, Griffin T T.. Abiraterone in metastatic prostate cancer. N Engl J Med. 368(15) (2013), 1458–9. [PubMed: 23574133]
4. Sumi T, Matsumoto K, Takai Y, Nakamura T.. Cofilin phosphorylation and actin cytoskeletal dynamics regulated by rho-and Cdc42-activated LIM-kinase 2. J. Cell Biol 147 (1999), 1519–32. [PubMed: 10613909]
5. Suyama E, Wadhwa R, Kawasaki H, Yaguchi T, Kaul SC, Nakajima M, et al. LIM kinase-2 targeting as a possible anti-metastasis therapy. J Gene Med. 6(3) (2004), 357–63. [PubMed: 15026997]

6. Vlecken DH, Bagowski CP. LIMK1 and LIMK2 are important for metastatic behavior and tumor cell-induced angiogenesis of pancreatic cancer cells. Zebrafish. 6(4) (2009), 433–9. [PubMed: 20047470]
7. Johnson EO, Chang KH, Ghosh S, Venkatesh C, Giger K, Low PS, et al. LIMK2 is a crucial regulator and effector of Aurora-A-kinase-mediated malignancy. J Cell Sci. 125, (2012), 1204–16. [PubMed: 22492986]
8. Nikhil K, Chang L, Viccaro K, Jacobsen M, McGuire C, Satapathy SR, et al. , Identification of LIMK2 as a therapeutic target in castration resistant prostate cancer. Cancer Lett. 448 (2019), 182–196. [PubMed: 30716360]
9. Awad D, Pulliam TL, Lin C, Wilkenfeld SR, Frigo DE. Delineation of the androgen-regulated signaling pathways in prostate cancer facilitates the development of novel therapeutic approaches. Curr Opin Pharmacol. 41 (2018), 1–11. [PubMed: 29609138]
10. Heemers HV. Androgen receptor and prostate cancer: new insights in an old target translate into novel therapeutic strategies. Curr Drug Targets. 14(4) (2013), 399–400. [PubMed: 23565752]
11. Zoubeidi A, Gleave ME. Co-targeting driver pathways in prostate cancer: two birds with one stone. EMBO Mol Med. 10(4) (2018), e8928. [PubMed: 29572264]
12. McMenamin ME, Soung P, Perera S, Kaplan I, Loda M, Sellers WR. Loss of PTEN expression in paraffin-embedded primary prostate cancer correlates with high Gleason score and advanced stage. Cancer Res. 59(17) (1999), 4291–96. [PubMed: 10485474]
13. Leinonen KA, Saramaki OR, Furusato B, Kimura T, Takahashi H, Egawa S, et al H., Loss of PTEN is associated with aggressive behavior in ERG-positive prostate cancer. Cancer Epidemiol Biomarkers Prev. 22(12) (2013), 2333–44. [PubMed: 24083995]
14. Myers MP, Stolarov JP, Eng C, Li J, Wang SI, Wigler MH, Parsons R, Tonks NK. PTEN, the tumor suppressor from human chromosome 10q23, is a dual-specificity phosphatase. Proc Natl Acad Sci USA 94 (1997), 9052–57. [PubMed: 9256433]
15. Maehama T, Dixon JE. The tumor suppressor, PTEN/MMAC1, dephosphorylates the lipid second messenger, phosphatidylinositol 3,4,5-trisphosphate. J Biol Chem 273 (1998), 13375–78. [PubMed: 9593664]
16. Mulholland DJ, Tran LM, Li Y, Cai H, Morim A, Wang S, Plaisier S, et al. Cell autonomous role of PTEN in regulating castration-resistant prostate cancer growth. Cancer Cell. 19 (2011), 792–804. [PubMed: 21620777]
17. Ham WS, Cho NH, Kim WT, Ju HJ, Lee JS, Choi YD. Pathological effects of prostate cancer correlate with neuroendocrine differentiation and PTEN expression after bicalutamide monotherapy. J Urol. 182 (2009), 1378–84. [PubMed: 19683286]
18. Lotan TL, Wei W, Morais CL, Hawley ST, Fazli L, Hurtado-Coll A, et al. PTEN loss as determined by clinical-grade immunohistochemistry assay is associated with worse recurrence-free survival in prostate cancer. Eur Urol Focus. 2 (2016), 180–8. [PubMed: 27617307]
19. Ferraldeschi R, Nava Rodrigues D, Riisnaes R, Miranda S, Figueiredo I, Rescigno P, et al. PTEN protein loss and clinical outcome from castration-resistant prostate cancer treated with abiraterone acetate. Eur Urol. 67(4) (2015), 795–802. [PubMed: 25454616]
20. Kim JS, Lee C, Bonifant CL, Ressom H, Waldman T.. Activation of p53-dependent growth suppression in human cells by mutations in PTEN or PIK3CA. Mol Cell Biol. 27(2) (2007), 662–77. [PubMed: 17060456]
21. Wang J, Nikhil K, Viccaro K, Lei C, White J, Shah K.. Phosphorylation-dependent Regulation of ALDH1A1 by Aurora Kinase A: Insights on their Synergistic Relationship in Pancreatic Cancer. BMC Biol. 15(1) (2017), 1–10. [PubMed: 28100223]
22. Johnson EO, Chang KH, de Pablo Y, Ghosh S, Mehta R, Badve S, et al. PHLDA1 is a Crucial Negative Regulator and Effector of Aurora A Kinase in Breast Cancer. J Cell Sci. 124 (2011), 2711–2722. [PubMed: 21807936]
23. Sun KH, Lee HG, Smith MA, Shah K.. Direct and Indirect Roles of Cdk5 as an Upstream Regulator in the JNK Cascade: Relevance to Neurotoxic Insults in Alzheimer's Disease. Mol Biol Cell. 20(21) (2009), 4611–9. [PubMed: 19776350]
24. Shah K, Vincent F.. Divergent roles of c-Src in controlling platelet-derived growth factor-dependent signaling in fibroblasts. Mol Biol Cell. l (11) (2005), 5418–32.

25. Wang J, Nikhil K, Viccaro K, Lei C, Jacobsen M, Sandusky G, et al. Aurora A-Twist1 Axis Promotes Highly Aggressive Phenotypes in Pancreatic Carcinoma. J Cell Sci. 130(6) (2017), 1078–93. [PubMed: 28167680]
26. Goodwin NC, Cianchetta G, Burgoon HA, Healy J, Mabon R, Strobel ED, et al. Discovery of a Type III Inhibitor of LIM Kinase 2 That Binds in a DFG-Out Conformation. ACS Med Chem Lett. 6(1) (2014), 53–7. [PubMed: 25589930]
27. Hodakoski C, Fine B, Hopkins B, Parsons R.. Analysis of intracellular PTEN signaling and secretion. Methods. 77 (2015), 164–71. [PubMed: 25462559]
28. Shah K, Shokat KM. A Chemical Genetic Screen for Direct v-Src substrates reveals Ordered Assembly of a Retrograde Signaling Pathway. Chem Biol. 9(1) (2002), 35–47. [PubMed: 11841937]
29. Mezna M, Wong AC, Ainger M, Scott RW, Hammonds T, Olson MF. Development of a high-throughput screening method for LIM kinase-1 using a luciferase-based assay of ATP consumption. J Biomol Screen 17(4) (2017), 460–8.
30. Lagoutte E, Villeneuve C, Lafanechère L, Wells CM, Jones GE, Chavrier P, Rossé C.. LIMK Regulates Tumor-Cell Invasion and Matrix Degradation Through Tyrosine Phosphorylation of MT1-MMP. Sci Rep. 6 (2016), 24925. [PubMed: 27116935]
31. Lin HK, Hu YC, Lee DK, Chang C.. Regulation of androgen receptor signaling by PTEN (phosphatase and tensin homolog deleted on chromosome 10) tumor suppressor through distinct mechanisms in prostate cancer cells. Mol Endocrinol. 18 (2004), 2409–23. [PubMed: 15205473]
32. Walker SM, Leslie NR, M Perera N, Batty IH, Downes CP. The tumor-suppressor function of PTEN requires an N-terminal lipid-binding motif. Biochem J. 379 (2014), 301–7.
33. Vazquez F, Ramaswamy S, Nakamura N, Sellers WR. Phosphorylation of the PTEN tail regulates protein stability and function. Mol Cell Biol. 20 (2000), 5010–18. [PubMed: 10866658]
34. Torres J, Pulido R.. The tumor suppressor PTEN is phosphorylated by the protein kinase CK2 at its C terminus. Implications for PTEN stability to proteasome-mediated degradation. J Biol Chem. 276 (2001), 993–98. [PubMed: 11035045]
35. Maccario H, Perera NM, Davidson L, Downes CP, Leslie NR. PTEN is destabilized by phosphorylation on Thr366. Biochem J. 405 (2007), 439–44. [PubMed: 17444818]
36. Li Z, Dong X, Wang Z, Liu W, Deng N, Ding Y. et al. Regulation of PTEN by Rho small GTPases. Nat Cell Biol. 7 (2005), 399–404. [PubMed: 15793569]
37. Yim EK, Peng G, Dai H, Hu R, Li K, Lu Y, et al. Rak functions as a tumor suppressor by regulating PTEN protein stability and function. Can Cell 15 (2009), 304–14.

Highlights:

- PTEN was identified a direct target of LIMK2.
- LIMK2 phosphorylates PTEN at 5 sites, which both degrades and inhibits its activity.
- LIMK2 is the missing link between hypoxia and PTEN degradation.
- PTEN degrades LIMK2 in a feedback loop.

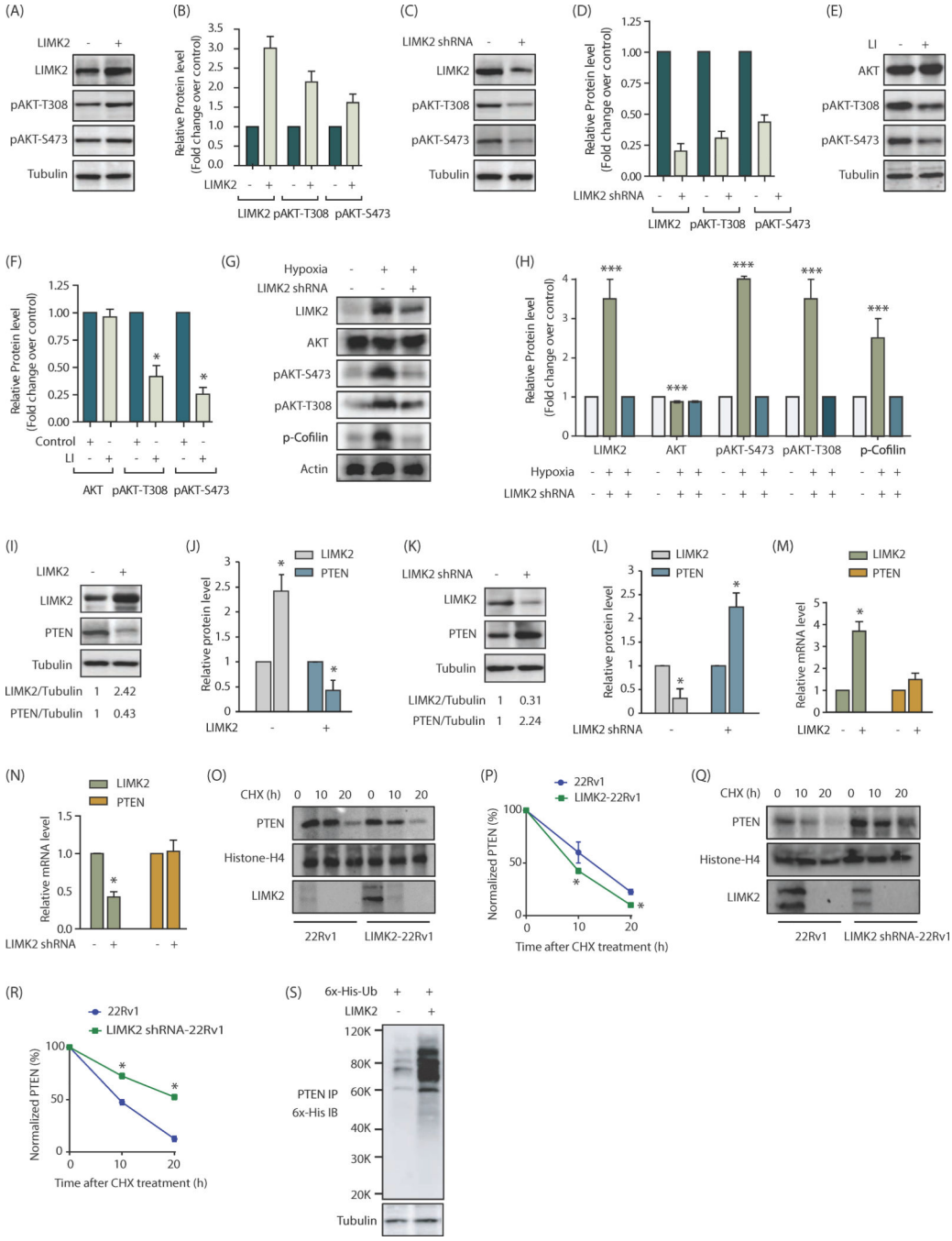

Figure 1:

LIMK2 upregulates PI3K signaling by stabilizing PTEN. (A) LIMK2 upregulates phosphorylation of AKT at S473 and T308 in 22Rv1 cells. (B) Bar graph shows increase in p-AKT level at T308 and S473 positions upon LIMK2 overexpression. The data shown are mean ± SEM of three independent experiments. (C) LIMK2 knockdown inhibits AKT phosphorylation in 22Rv1 cells. (D) Histogram shows change in AKT phosphorylation. The data represented as mean ± SEM of three independent experiments. *P <0.05 compared to control cells. (E) Change in AKT phosphorylation in response to LIMK2 inhibitor, LI.

22Rv1 cells were treated with 10 μM LI for 12h followed by immunoblot analysis. Each experiment was performed at least three independent times. Representative data are shown. (F) Bar graph shows change in p-AKT phosphorylation levels upon LI treatment. *P <0.05 compared to control cells. (G) LIMK2 and AKT protein and phosphorylation levels in hypoxia-induced 22Rv1 cells or LIMK2 shRNA-treated 22Rv1 cells. To induce hypoxia 22Rv1 cells were exposed to hypoxic conditions for 24h. For depleting LIMK2, LIMK2 shRNA was added 18h prior to hypoxia treatment. (H) Bar graph showing LIMK2, AKT, p-cofilin and p-AKT levels under normoxic and hypoxic conditions ± LIMK2 knockdown. The data shown are mean ± SEM of three independent experiments., ***P<0.0005 (I) LIMK2 inversely regulates PTEN levels in 22Rv1 cells. LIMK2 and PTEN levels were analyzed in LIMK2-overexpressing 22Rv1 and vector infected cells. (J) The bar graph shows relative band intensities of LIMK2 and PTEN from 22Rv1 and LIMK2–22Rv1 cells normalized to the corresponding tubulin levels. Data are expressed as fold change relative to control; values represented as mean ± SEM of three independent experiments. *P <0.05 compared to control cells. (K) LIMK2 knockdown increases PTEN levels in 22Rv1 cells. 22Rv1 cells were treated with either scrambled shRNA or LIMK2-shRNA, and LIMK2 and PTEN levels analyzed. (L) Histogram shows relative band intensities normalized to the corresponding tubulin level. Data shown as mean ± SEM of three independent experiment. *P <0.05 compared to control cells. (M) LIMK2 overexpression or (N) LIMK2 knockdown does not affect PTEN mRNA levels as analyzed by qPCR analysis. (O) LIMK2 augments PTEN degradation. 22Rv1 and LIMK2–22Rv1 cells were treated with cycloheximide (CHX, 10 μM) for 10h and 20h, and LIMK2 and PTEN levels analyzed. (P) Graphical representation of PTEN degradation rate in cells treated as in O, *P <0.05 compared to control cells. (Q) LIMK2 knockdown decelerate PTEN degradation. (R) Graphical representation of PTEN degradation rate in cells treated as in Q. *P <0.05 compared to control cells. (S) LIMK2 increases PTEN degradation by promoting its ubiquitylation. 22Rv1 cells were co-infected with 6x-His–ubiquitin (6x-His-Ub) along with LIMK2 overexpressing retrovirus for 30h, followed by a 12h MG132 treatment. PTEN proteins was immunoprecipitated and ubiquitylation analyzed using 6x-His antibody. Each experiment was done at least three independent times and representative data is shown.

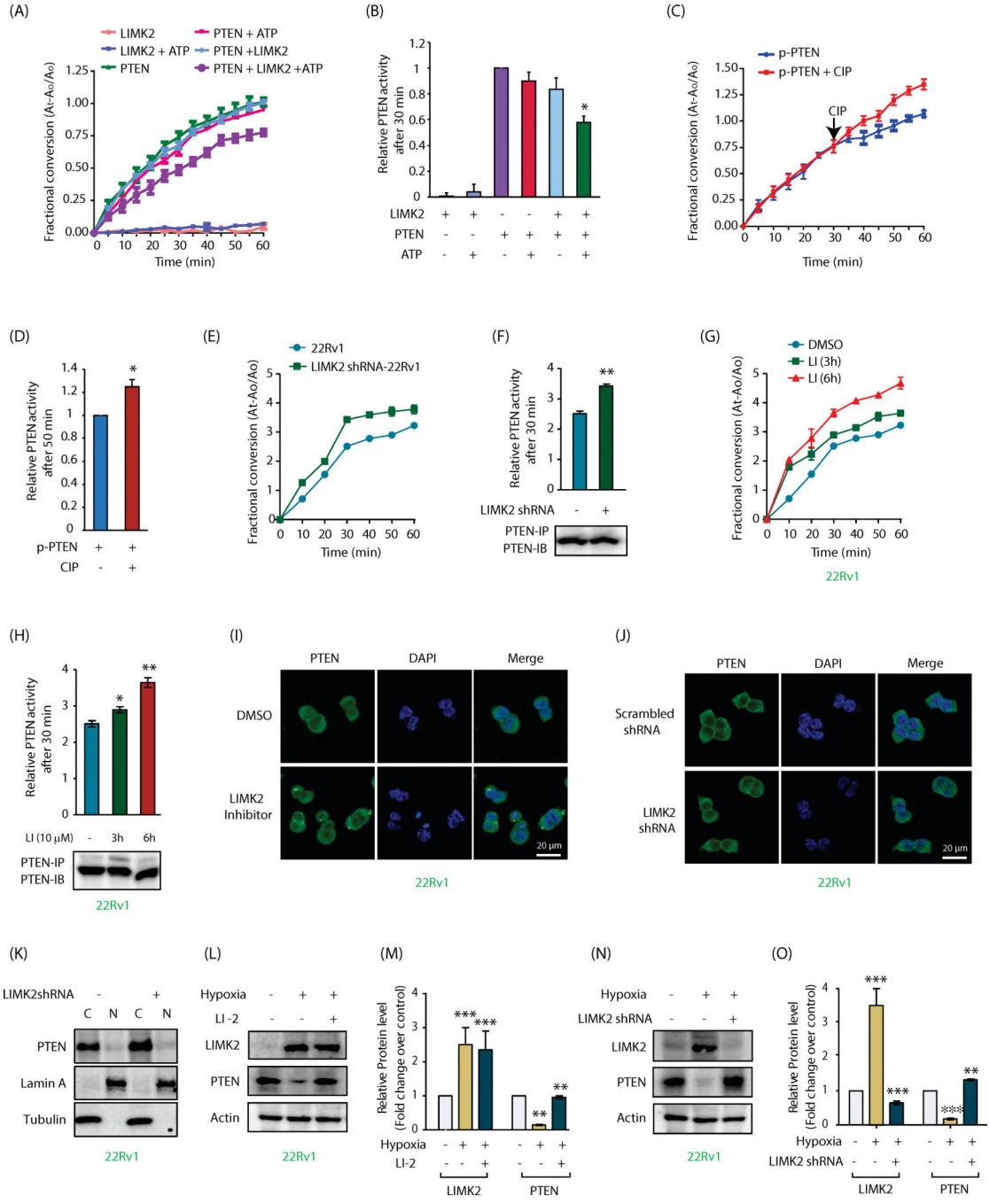

Figure 2:

LIMK2 inhibits PTEN phosphatase activity in vitro and in cells and downregulates its levels upon hypoxia. (A) LIMK2-mediated phosphorylation of PTEN decreases its phosphatase activity. PTEN was immunoprecipitated from 22Rv1 cell lysate and subjected to LIMK2 kinase assay. PTEN activity was calculated using PIP3 as a substrate. The signal was obtained by measuring the absorbance of free phosphate over time at 620 nm. (B) Same data as Figure 2A showing PTEN phosphatase activity at 30 min. (C) Dephosphorylation of PTEN by calf intestinal alkaline phosphatase (CIP) increases its phosphatase activity.

Each experiment was repeated three independent times. Representative data are shown. (D) Same data as Figure 2C showing PTEN phosphatase activity at 50 min. (E) LIMK2 knockdown augments PTEN phosphatase activity in 22Rv1 cells. (F) Same data as Figure 2E showing PTEN phosphatase activity at 30 min along with immunoblots showing loading control of PTEN for each reaction, **P<0.005. (G) Treatment with 10 μM LIMK2 inhibitor for 3 and 6 h increases PTEN activity in 22Rv1 cells. (H) Quantification of data in Figure 2G showing PTEN phosphatase activity at 45 min. *P<0.05, **P<0.005 (I) Immunofluorescence analysis to detect PTEN localization in response to LIMK2 inhibitor in 22Rv1 cells. (J) Immunofluorescence analysis to detect PTEN localization in response to LIMK2 knockdown in 22Rv1 cells. (K) Subcellular fractionation of PTEN in 22Rv1 and LIMK2 shRNA-treated 22Rv1 cells. Alpha-tubulin and lamin A are the cytoplasmic marker and nuclear marker, respectively. N, nuclear fraction; C, cytoplasmic fraction. (L) LIMK2 negatively regulates PTEN protein level under hypoxic conditions. LIMK2 inhibition using LI rescues the loss of PTEN. (M) LIMK2 and PTEN protein levels in hypoxia facing 22Rv1 cells in presence and absence of LIMK2 inhibitor. Data shown are mean ± SEM of three independent experiments. **P < 0.005, ***P<0.0005 vs control cells. (N) Effect of hypoxia on PTEN protein levels in the presence and absence of LIMK2 shRNA. (O) Bar graph shows LIMK2 and PTEN protein levels in cobalt chloride ± LIMK2 shRNA cells. *P < 0.05 vs control cells.

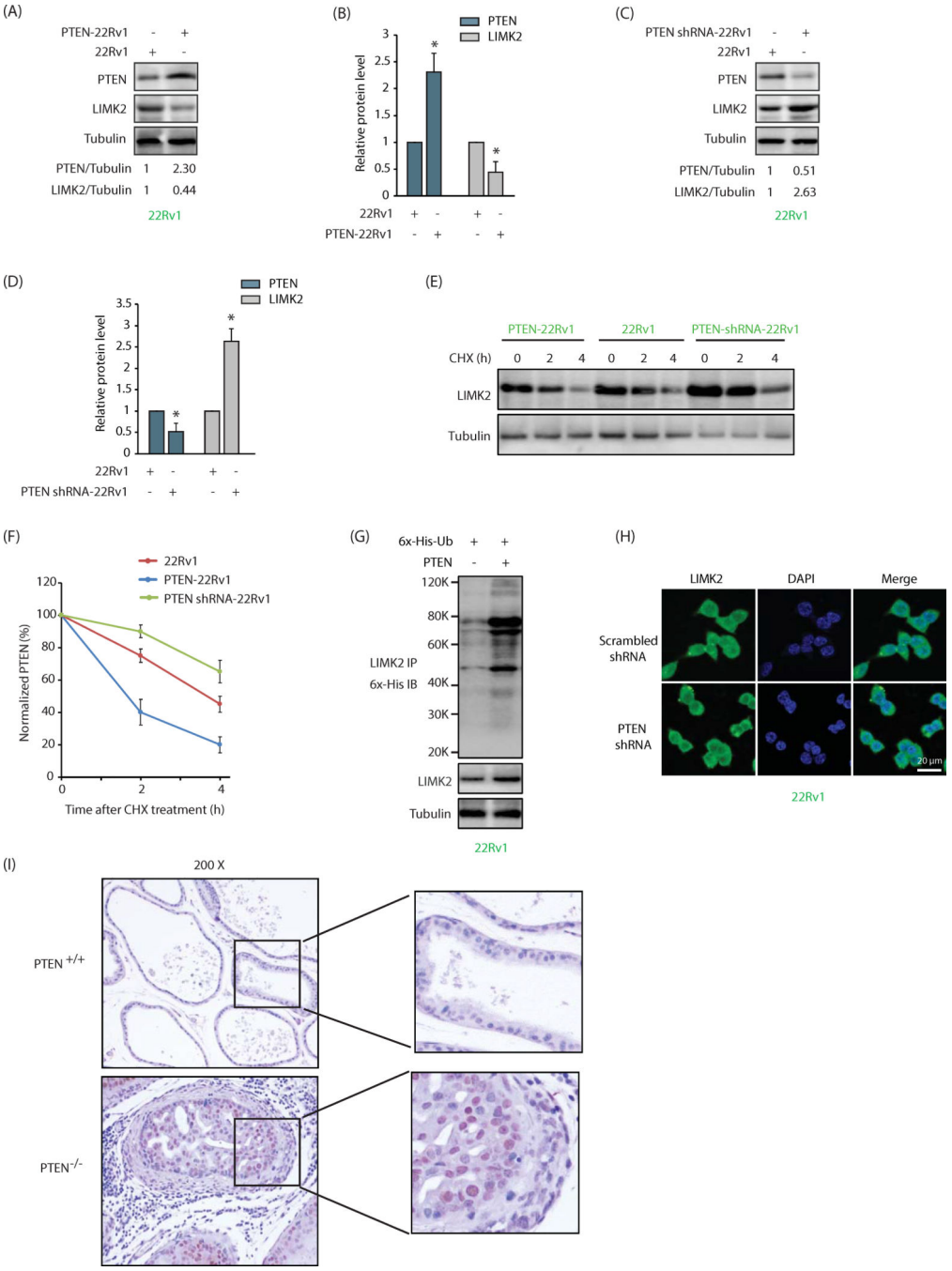

Figure 3:

PTEN engages in a negative feedback loop with LIMK2. (A) PTEN overexpression depletes LIMK2 protein in 22Rv1 cells. (B) Histogram shows relative band intensities of PTEN and LIMK2 normalized to the corresponding tubulin level. Data shown are mean ± SEM of three independent experiments. *P <0.05 compared to control cells. (C) PTEN knockdown increases LIMK2 levels in 22Rv1 cells. (D) Histogram shows relative band intensities normalized to the corresponding tubulin level. Data shown as mean ± SEM of three independent experiment. (E) PTEN accelerates LIMK2 degradation. 22Rv1, PTEN-22Rv1

and PTEN shRNA-22Rv1 cells were treated with cycloheximide (CHX) for 2 and 4h, and LIMK2 levels analyzed. (F) Graphical representation of PTEN degradation rate. (G) PTEN degrades LIMK2 by promoting its ubiquitylation. Each experiment was repeated at least three independent times and a representative data is shown. (H) PTEN knockdown does not alter LIMK2 localization in 22Rv1 cells. (I) LIMK2 levels are higher in prostates from $PTEN^{-/-}$mice as compared to prostates from $PTEN^{+/+}$ mice. Diaminobenzidine staining of LIMK2 in prostate tissues of wild-type $PTEN^{+/+}$ and homozygous depleted PTEN $^{-/-}$ mice at the age of 3 months. PTEN was depleted in a prostate-specific manner.

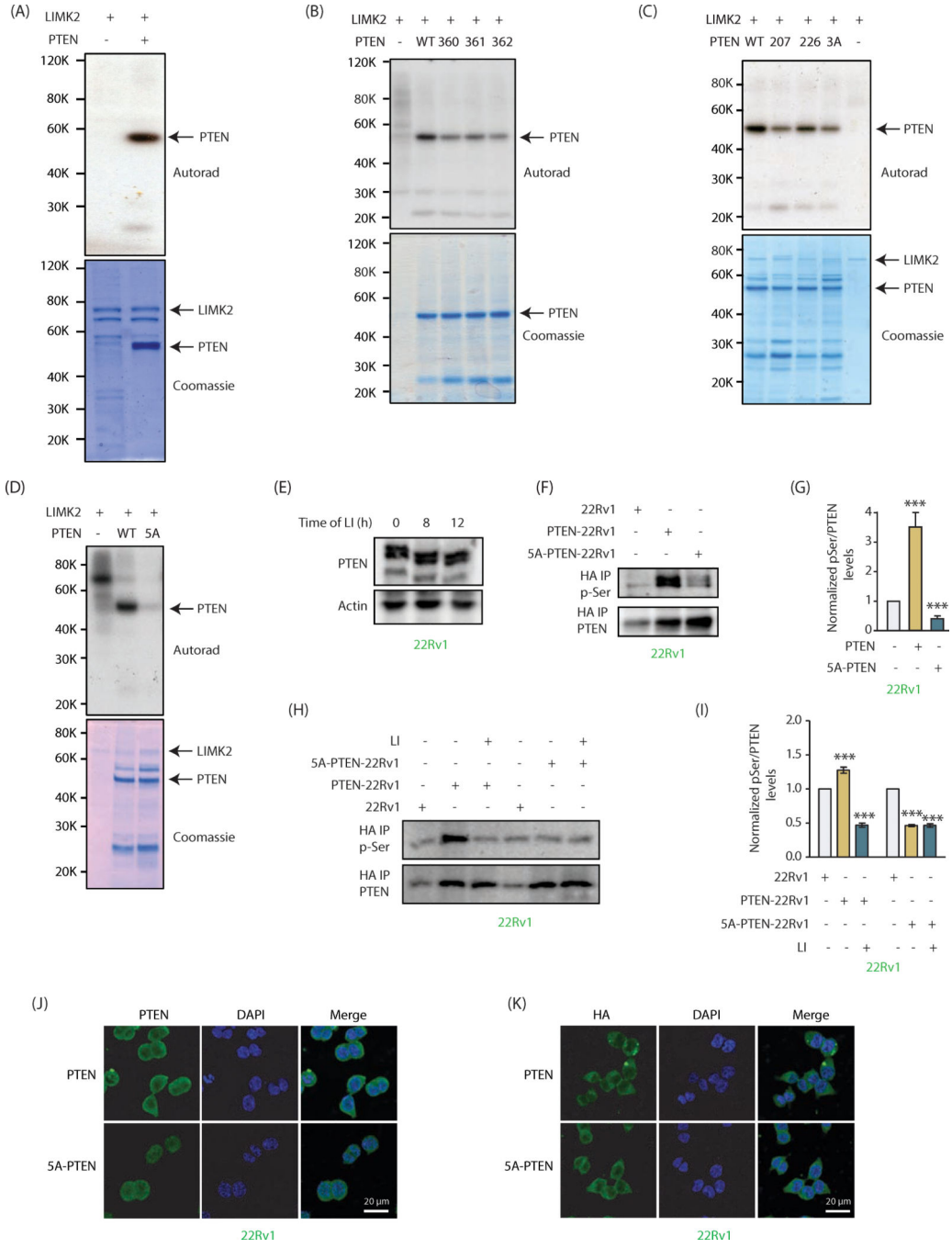

Figure 4:

PTEN is directly phosphorylated by LIMK2 at five sites (A) LIMK2 directly phosphorylates PTEN. Lane 1 contains [^{32}P]ATP and LIMK2 and lane 2 contains 6x-His-PTEN, LIMK2 and [^{32}P]ATP. Kinase reaction was conducted for 30 minutes. The lower panel shows LIMK2 and PTEN Coomassie staining of the same gel. (B) LIMK2 phosphorylates PTEN at S360, S361 and S362 sites. WT and single mutants of PTEN at S360, S361 and S362 sites were subjected to in vitro kinase assay using LIMK2 and [^{32}P]ATP. (C) LIMK2 phosphorylates PTEN at S207, S226 and 3A sites (S360/S361/S362). The corresponding

phospho-resistant single mutants (S207A, S226A) and triple mutant S3A (360A, S361A and S362A) were generated and subjected to *in vitro* kinase assay using LIMK2. The top panel shows autoradiography, and lower panel shows LIMK2 and PTEN Coomassie stains. (D) LIMK2 phosphorylates PTEN at only above-mentioned five sites (S207, S226, S360, S361 and S362), as the corresponding 5A-phospho-resistant mutant did not show any phosphorylation. (E) Mobility shift analysis of PTEN phosphorylation in intact cells. LIMK2 was inhibited in 22Rv1 cells using LIMK2 inhibitor (LI, 10 μM) for 8h and 12h and lysates were run on 10% SDS-PAGE gel followed by immunoblotting using PTEN antibody. (F) Ectopically expressed WT and 5A-PTEN were immunoprecipitated using HA antibody and assayed for phospho-serine levels. (G) Quantification of blots obtained from three independent experiments in part F reveal a significant loss of phosphorylation in case of the 5A mutant, ***P<0.0005. (H) Phospho-serine levels were also assayed with and without inhibition of LIMK2 (10 μM LI, 12h) in both PTEN-22Rv1 and 5A-PTEN-22Rv1 cells. (I) Quantification of data obtained for part H shows minimal phosphorylation of 5A-PTEN. Furthermore, phospho-levels of 5A-PTEN remain unchanged by LIMK2 inhibition confirming that these are the only sites of phosphorylation by LIMK2. Graph represents data obtained from three independent experiments. These are shown as mean ± SEM with ***P <0.0005 compared to control cells. (J) Subcellular localization of PTEN in PTEN-22Rv1 and 5A-PTEN-22Rv1 cells. (K) PTEN and 5A-mutant showed similar subcellular localization when analyzed using HA antibody.

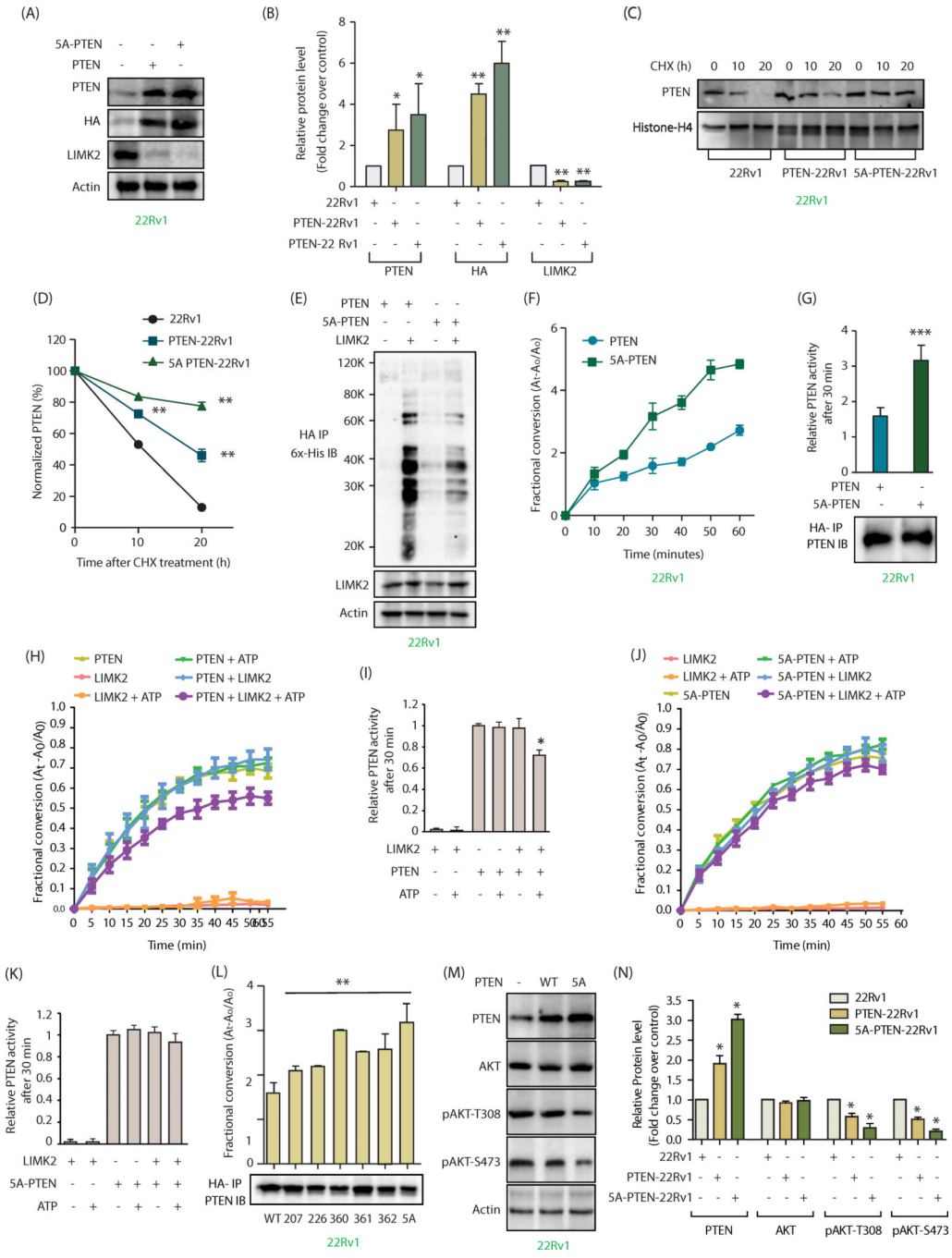

Figure 5:

LIMK2-mediated phosphorylation is responsible for increased ubiquitylation and inhibition of PTEN activity, causing AKT activation. (A) Phospho-resistant PTEN is expressed at higher levels compared to WT-PTEN in 22Rv1 cells. 22Rv1 cells were infected with HA-tagged wild-type PTEN or 5A-PTEN retrovirus for 36h, and protein levels of PTEN, LIMK2, HA and actin were analyzed using their respective antibodies. (B) The bar graph shows average values of wild type and mutant PTEN obtained from three independent experiments. Data shown are mean ± SEM of three independent experiments.

*P <0.05, **P<0.005 compared to control cells. (C) LIMK2-mediated phosphorylation of PTEN decreases its stability. PTEN levels were analyzed in 22Rv1, PTEN-22Rv1 and 5A-PTEN-22Rv1 cells treated with cycloheximide for 10 and 20h. (D) Graphical representation of PTEN half-life in 22Rv1, PTEN-22Rv1 and 5A-PTEN-22Rv1 cells.**P<0.005. (E) LIMK2 overexpression significantly increased the ubiquitylation of WT-PTEN, as compared to 5A-PTEN in 22Rv1 cells. WT PTEN-22Rv1 and 5A-PTEN-22Rv1 cells were infected with 6x-His-Ubiquitin with or without LIMK2 retrovirus for 30h, followed by MG132 treatment for 12h. PTEN was immunoprecipitated using HA antibody and ubiquitylation analyzed using 6x-His antibody. (F) Phospho-resistant PTEN has increased phosphatase activity as compared to WT-PTEN. (G) Same data as Figure 5F showing PTEN phosphatase activity at 30 min in WT-PTEN-22Rv1 and 5A-PTEN-22Rv1 cells along with PTEN loading control. (H) LIMK2-mediated phosphorylation of PTEN decreases its phosphatase activity. PTEN was expressed and purified from SF9 insect cells and subjected to LIMK2 kinase assay. PTEN activity was calculated by measuring the absorbance of free phosphate over time at 620 nm using PIP3 as a substrate. (I) Same data as Figure 5H showing PTEN phosphatase activity at 30 min. (J) Phospho-resistant PTEN showed no significant change in phosphatase activity. (K) Same data as Figure 5J showing PTEN phosphatase activity at 30 min. Data obtained from three independent experiments was plotted as mean ± SEM of with *P <0.05 compared to control cells and **P<0.005 compared to control cells. (L) Effect of LIMK2-mediated phosphorylation on PTEN activity. Single mutants for each phosphorylation site were ectopically expressed in 22Rv1 cells and immunoprecipitated using HA antibody, phosphatase activity was assayed as before at 30 minutes and immunoblot for PTEN loading control is also shown. **P<0.005 compared to control cells. (M) Change in AKT phosphorylation in WT and 5A-PTEN cells. (N) Histogram shows change in AKT phosphorylation level in response to WT or 5A-PTEN expression. The data represented as mean ± SEM of three independent experiments. *P <0.05 compared to control cells.

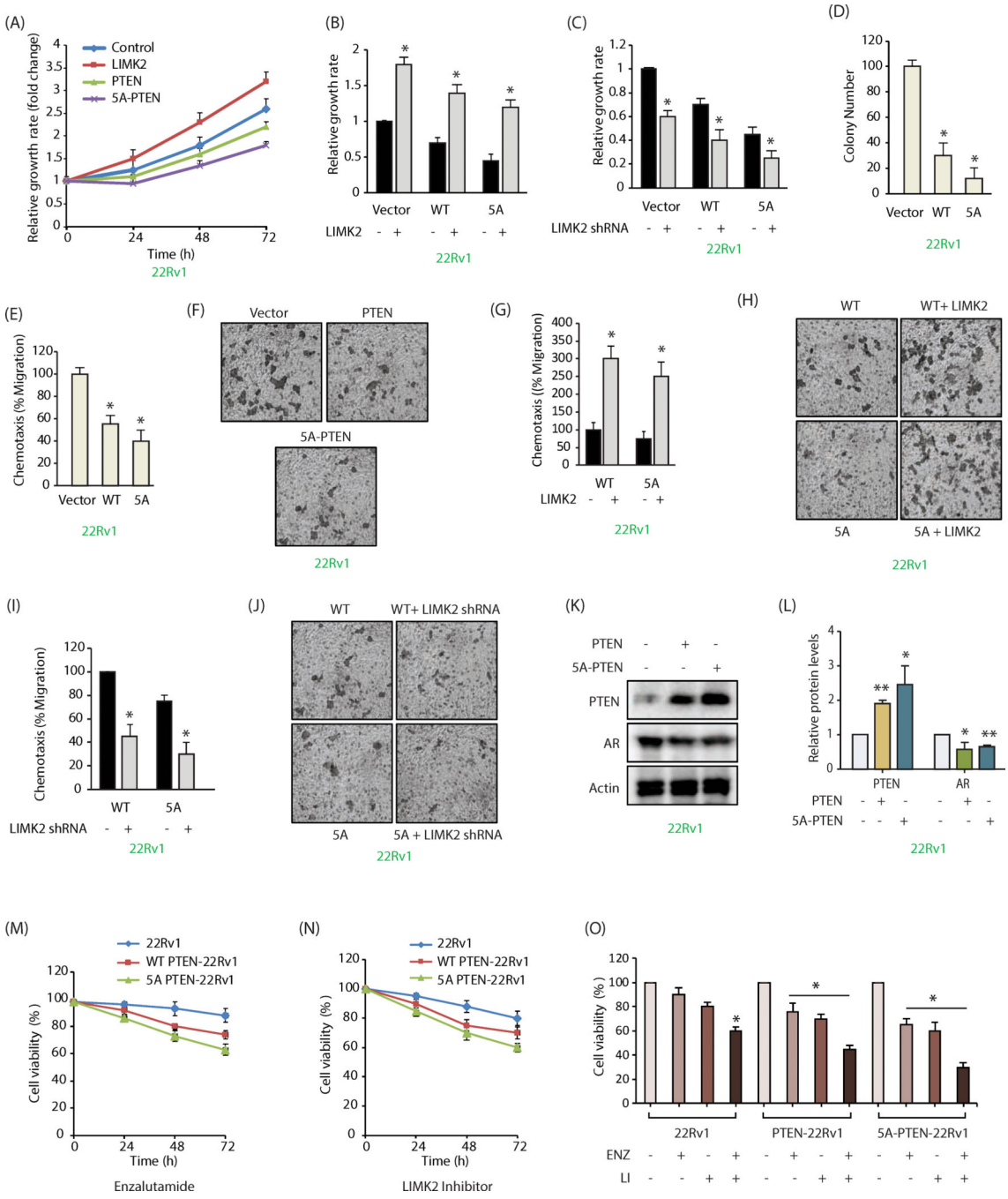

Figure 6:

LIMK2-mediated phosphorylation of PTEN contributes to aggressive oncogenic phenotypes in 22Rv1 cells. (A) Expression of WT and 5A-PTEN impaired cell proliferation in 22Rv1 cells. 22Rv1, LIMK2–22Rv1, PTEN-22Rv1 and 5A-PTEN-22Rv1 cells were cultured in 96-well plates for 24, 48, and 72h and subjected to MTT assay. (B) Data showing increased cell proliferation in 22Rv1, PTEN-22Rv1 and 5A-PTEN-22Rv1 cells upon LIMK2 overexpression. (C) LIMK2 depletion substantially reduced cell growth in 22Rv1, PTEN-22Rv1 and 5A-PTEN-22Rv1 cells. (D) 5A-PTEN shows maximal inhibition of

colony formation in a soft agar assay in 22Rv1 cells. *P < 0.05 compared to vector-expressing control analyzed by one-way ANOVA. (E) PTEN and 5A-PTEN inhibit cell migration in 22Rv1 cells. Chemotaxis assay was performed in 22Rv1, PTEN-22Rv1 and 5A-PTEN-22Rv1 cells using Boyden chambers. Histogram shows mean ± SEM of three independent experiments. *P < 0.05 compared to vector control. (F) Representative images of chemotaxis assay. Magnification, 200×. (G and H) LIMK2 overexpression increases cell motility in both PTEN-22Rv1 and 5A-PTEN-22Rv1 cells. (I and J) LIMK2 depletion inhibits cell motility in both PTEN-22Rv1 and phospho-resistant 5A-PTEN-22Rv1 cells. (K) Variation in AR levels in response to PTEN as assayed using ectopic expression of WT and 5A PTEN. *P < 0.05, **P < 0.005. (L) Quantification of data shows significant decrease in AR levels in both WT and 5A-mutant expressing cells. (M) LIMK2-mediated phosphorylation of PTEN increases enzalutamide-sensitivity. 22Rv1, PTEN-22Rv1 and 5APTEN-22Rv1 cells were plated overnight, enzalutamide (1 μM) was added and cells were grown for additional 24, 48 or 72h, followed by MTT assay. (N) PTEN overexpression increases LIMK2 inhibitor sensitivity in 22Rv1 cells. 22Rv1, PTEN-22Rv1 and 5A-PTEN-22Rv1cells were plated overnight, followed by LIMK2 inhibitor (10 μM) treatment. The cells were grown for additional 24, 48 or 72h, followed by MTT assay. (O) 5A-PTEN overexpression sensitizes 22Rv1 cells to LIMK2 inhibitor and enzalutamide, 22Rv1, PTEN-22Rv1 and 5A-PTEN-22Rv1cells were plated overnight, followed by enzalutamide (1 μM) or LIMK2 inhibitor (10 μM) treatments either independently or in combination. The cells were grown for additional 72h, followed by MTT assay.

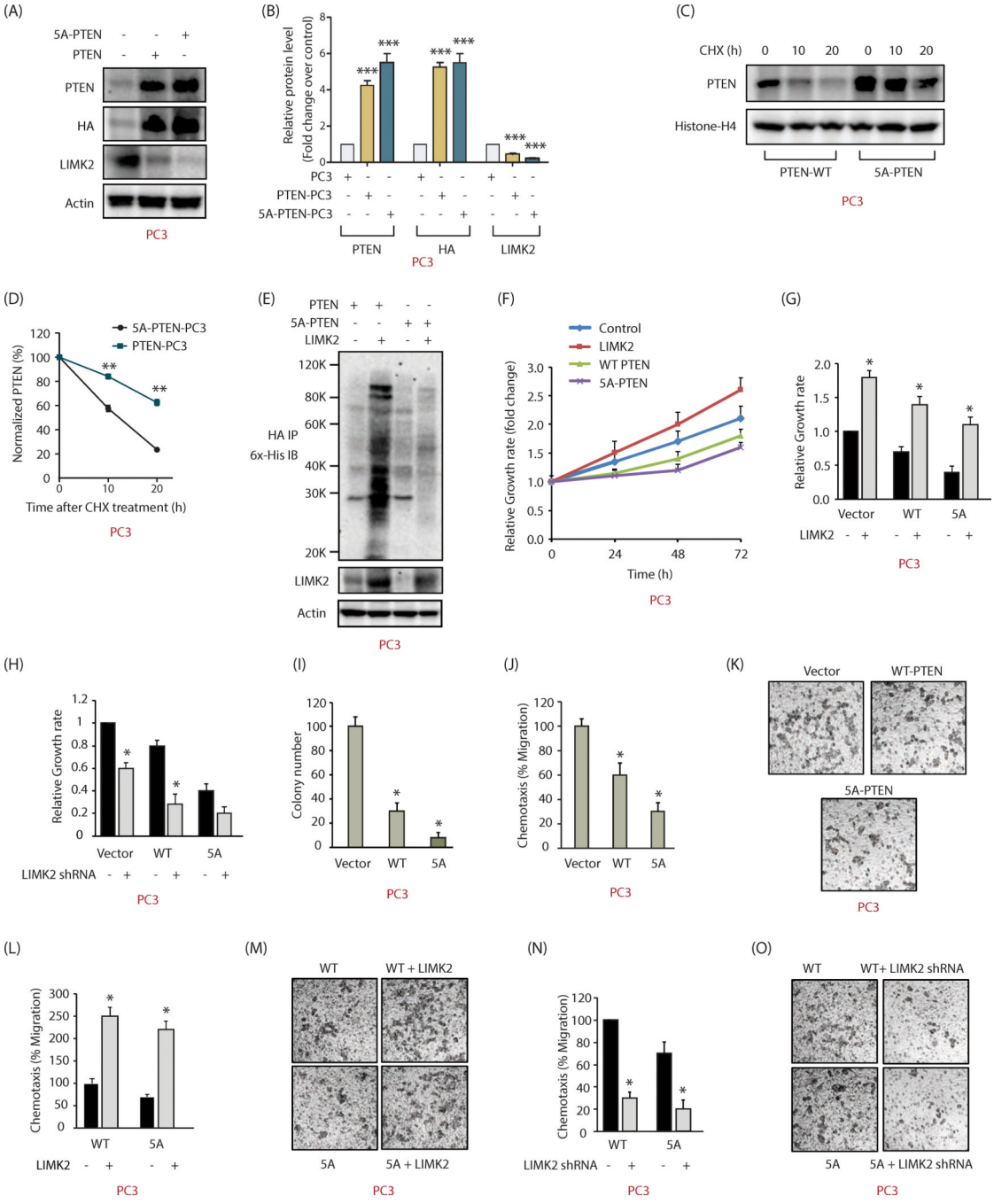

Figure 7:

LIMK2 destabilizes PTEN in PC3 cells and promotes metastatic phenotypes. (A) 5A-PTEN is expressed at higher-level compared to WT-PTEN in PTEN-deficient PC3 cells. HA-tagged wild-type PTEN or 5A-PTEN were ectopically expressed in PC3 cells and protein levels of PTEN, LIMK2 and actin were analyzed using their respective antibodies. (B) Histogram shows average values of wild type and mutant PTEN obtained from three independent experiments. Data shown are mean ± SEM. ***P <0.0005 as compared to control cells. (C) LIMK2-mediated phosphorylation of PTEN decreases its stability. PTEN levels were

analyzed in PTEN-PC3 and 5A-PTEN-PC3 cells treated with cycloheximide (10 μM) for 10 and 20h. (D) Graphical representation of PTEN half-life in PTEN-PC3 and 5A-PTEN-PC3 cells. **P <0.005. (E) LIMK2 overexpression increased the ubiquitylation of WT-PTEN, but not 5A-PTEN in PC3 cells. (F) Expression of WT and 5A-PTEN impaired cell proliferation in PC3 cells. PC3, LIMK2-PC3, PTEN-PC3 and 5A-PTEN-PC3 cells were cultured in 96-well plates for 24, 48, and 72h and subjected to MTT assay. (G) Data showing increased cell proliferation in PTEN-PC3 and 5A-PTEN-PC3 on LIMK2 overexpression. (H) LIMK2 depletion substantially reduced cell growth in PTEN-PC3 and 5A-PTEN-PC3 cells. (I) PTEN prevents colony formation in a soft agar assay in PC3 cells. *p < 0.05 as compared to vector-expressing control. (J) PTEN inhibits cell motility in PC3 cells. *p < 0.05 as compared to vector control. (K) Representative images of chemotaxis assay, Magnification, 200×. (L and M) LIMK2 overexpression increases cell motility in both PTEN-PC3 and 5A-PTEN-PC3 cells. (N and O) LIMK2 depletion inhibits cell motility in both PTEN-PC3 and phospho-resistant 5A-PTEN-PC3 cells.

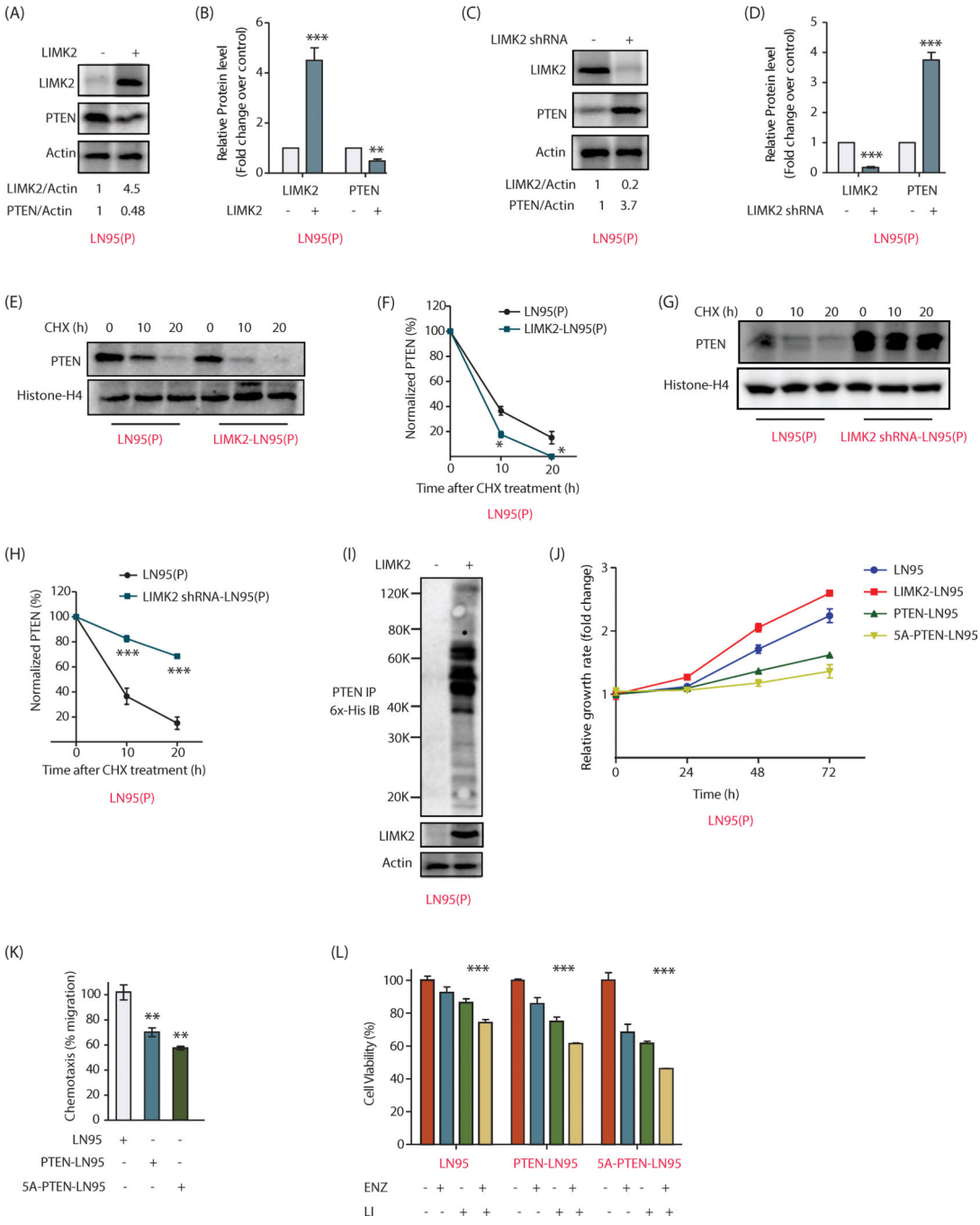

Figure 8:

LIMK2 destabilizes PTEN in LN95 cells and promotes metastatic phenotypes. (A) Overexpression of LIMK2 severely decreases the levels of ectopically expressed PTEN in LN95 cells. (B) Bar graph representation of data from three independent experiments. Data shown are mean ± SEM. ***P <0.0005 compared to control cells. (C) LIMK2 knockdown increased PTEN levels in LN95 cells. (D) Quantification of protein levels shows significantly high levels of PTEN in LIMK2 knockdown cells. ***P <0.0005 compared to control cells. (E) Stability of PTEN was analyzed in LN95(P) and LIMK2 overexpressing

LN95(P) cells using cycloheximide treatment (10 μM) for 10 and 20h. (F) Graphical representation of the half-life of PTEN in LN95(P) and LIMK2 overexpressing LN95(P) cells. **P <0.005 compared to control cells. (G) Cycloheximide chasing of PTEN in LN95(P) and LIMK2 knockdown LN95(P) cells. (H) Quantitative analysis of data obtained from three independent experiments revealed significantly higher stability of PTEN in LIMK2 depleted cells. **P <0.005 compared to control cells. (I) LIMK2 overexpression increased the ubiquitylation of PTEN in LN95(P) cells. (J) Expression of WT and 5A-PTEN impaired cell proliferation in LN95 cells. (K) PTEN inhibits migratory ability of LN95 cells. **P < 0.005 compared to vector control. (L) 5A-PTEN overexpression sensitizes LN95 cells to LIMK2 inhibitor and enzalutamide, with the combination of the two significantly lowering the cell viability.

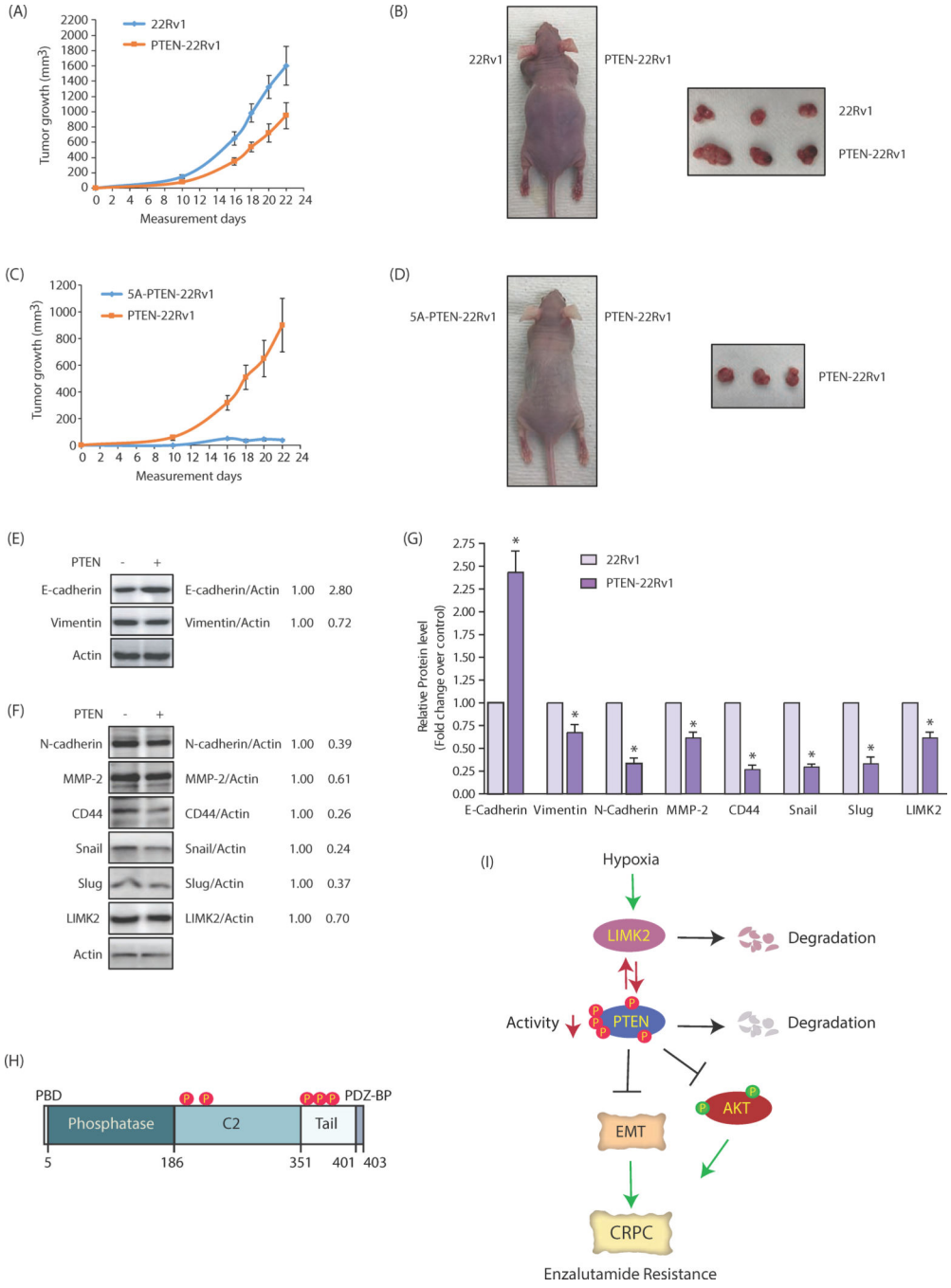

Figure 9:

PTEN phosphorylation and downregulation by LIMK2 promotes tumorigenesis and EMT in vivo. (A) PTEN overexpression reduces tumor growth *in vivo*. Three male athymic nude mice were inoculated with equal number of 22Rv1 and PTEN-22Rv1 cells on left and right shoulders, respectively. The mean value ± SEM. were obtained from three animals in each group. (B) Photograph of mouse and tumors derived from 22Rv1 cells and PTEN-22Rv1 cells in nude mice. Pictures were taken 23 days following injection. (C) Effect of 5A-PTEN expression on subcutaneous tumor growth in athymic nude mice. Three

nude mice were inoculated with PTEN-22Rv1 and 5A-PTEN-22Rv1 cells on the right and left shoulders, respectively. (D) Athymic nude mouse injected with PTEN-22Rv1 cells and 5A-PTEN-22Rv1 on right and left shoulders. The pictures were taken 23 days following inoculation. A representative image is presented. (E) and (F) Western blot analysis to show change in levels of LIMK2, EMT and CSC markers with PTEN overexpression in the tumors of nude mice. (G) Quantitative change in protein level of EMT and CSC marker. Data shown as mean ± SEM of three independent experiments. *$p < 0.05$ compared to vector control. (H) Domain structure of PTEN with the five phosphorylation sites identified in this study. (I) Overall regulatory mechanism depicting the involvement of LIMK2 and PTEN in CRPC progression.